

IL NUOVO CIMENTO
DOI 10.1393/ncc/i2005-10064-x

VOL. 28 C, N. 6

Novembre-Dicembre 2005

The no-slip condition at the western boundary of a homogeneous ocean minimizes energy

F. CRISCIANI⁽¹⁾(*) and F. CAVALLINI⁽²⁾(**)

⁽¹⁾ *CNR-Istituto di Scienze Marine
viale Romolo Gessi 2, I-34123 Trieste, Italy*

⁽²⁾ *Istituto Nazionale di Oceanografia e di Geofisica Sperimentale-OGS
Borgo Grotta Gigante 42/C, I-34010 Sgonico (Trieste), Italy*

(ricevuto il 20 Giugno 2005; approvato il 20 Ottobre 2005; pubblicato online il 18 Gennaio 2006)

Summary. — It is not obvious, *a priori*, that the no-slip boundary condition is suitable for ocean circulation models based on quasi-geostrophic equations. But the no-slip condition is the one that minimizes the kinetic energy of the western boundary layer of a wind-driven ocean governed by fourth-order quasi-geostrophic equations. Moreover, the case of a very thin boundary layer is correctly described by the asymptotic solution when the no-slip condition is chosen. Then, it is physically sound to use the no-slip condition even in the western boundary of analytical or numerical ocean circulation models, be they linear or nonlinear.

PACS 92.10.Fj – Dynamics of the upper ocean.

1. – Introduction

The so-called no-slip condition expresses, by definition, the continuity of the tangential component of velocity across the boundary separating a fluid and a solid. According to Batchelor [1], at the level of molecular interaction “*the absence of slip at a rigid wall is amply confirmed by direct observation and by the correctness of its many consequences under normal conditions*”. However, in the framework of ocean dynamics, Pedlosky [2] observes that it is not clear that no-slip condition “*is the correct boundary condition when our equations explicitly resolve only the large-scale motion. The no-slip condition is a reflection of the interaction of the fluid with a solid boundary on the microscopic level, and there is no reason why motion on scales of the order of hundreds or thousands of kilometers should mimic that interaction*”.

(*) E-mail: fulvio.criscianni@ts.ismar.cnr.it

(**) E-mail: fcavallini@ogs.trieste.it

Given the present difficulty in resolving in a deductive way the validity of the no-slip condition in large-scale motion (see, for instance, also Kamenkovich *et al.* [3] and Mc Williams [4]), a distinctive flow property that comes from the no-slip condition can be useful to accept or reject the latter, for instance in setting up a circulation model. To this purpose, we investigate the quasi-geostrophic dynamics, in the western boundary layer of an idealized basin, of a homogeneous wind-driven flow field in frictional regimes governed by the nondimensional steady vorticity equation

$$(1) \quad \frac{\partial \psi}{\partial x} = \text{curl}_z \bar{\tau} - \frac{\delta_s}{L} \nabla^2 \psi + \left(\frac{\delta_M}{L} \right)^3 \nabla^4 \psi$$

in the square fluid domain

$$(2) \quad D = [0 \leq x \leq 1] \times [0 \leq y \leq 1] ,$$

where standard notation is understood, and the usual no mass-flux boundary condition is assumed (*e.g.*, Pedlosky [5]).

It is known that, if no further boundary condition (so-called additive) is applied to the flow in the presence of lateral diffusion of relative vorticity (*i.e.* for $\delta_M > 0$), then the solution of (1) is not unique but, within the boundary layer approximation, the related streamfunction ψ depends on an arbitrary function of latitude, say $C(y)$. On this subject, recent results have been obtained by Castellana *et al.* [6] and Crisciani [7]. We stress that the boundary layer approach has the noticeable feature to make explicit and continuous, through the function $C(y)$, the dependence of the model solution on the additive boundary conditions. Thus, one may avoid to compare different solutions between them, each being characterized by a definite additive boundary condition assumed *a priori*.

In this paper we consider the total kinetic energy of the flow in the whole western boundary layer of nondimensional width δ_F/L , where

$$(3) \quad \delta_F = \max(\delta_S, \delta_M) ,$$

and we show that this energy has a unique minimum, which corresponds to the function $C(y)$ that selects the no-slip condition at the western boundary. Further, we interpret this minimum-energy property as an argument supporting the physical soundness of the no-slip condition even in large-scale circulation models. Finally, we argue that the no-slip condition should be used also with the nonlinear version of (1) since, at least in all the circulation models conceived up to now, the dynamic boundary conditions have been assumed to be independent of linearity/nonlinearity assumptions.

2. – Formulation of the problem

To prove the statement claimed in the last paragraph of the introduction, we resort to the well-known boundary layer approximation applied to the streamfunction in the proximity of the western wall of the considered basin. Only suitably nondimensionalized quantities are considered. With reference to (1) and (2), the superposition

$$(4) \quad \psi^{(w)} = \psi_I(x, y) + \phi(\xi, y)$$

is assumed, where ψ_I is the interior component that comes from the Sverdrup balance in the presence of the wind-stress field $\bar{\tau}(x, y)$, *i.e.*

$$(5) \quad \psi_I(x, y) = - \int_x^1 \text{curl}_z \bar{\tau}(x', y) dx',$$

while

$$(6) \quad \phi(\xi, y)$$

is the correction term that constitutes the object of our investigation. In (6)

$$(7) \quad \xi = \frac{L}{\delta_F} x$$

is the stretched coordinate relative to the frictional boundary layer width δ_F . With reference to (3), note that δ_S/L and δ_M/L are the nondimensional widths of the Stommel and Munk layers, respectively. Function (6) is a solution of the problem

$$(8) \quad \begin{aligned} \left(\frac{\delta_M}{\delta_F}\right)^3 \frac{\partial^3 \phi}{\partial \xi^3} - \frac{\delta_S}{\delta_F} \frac{\partial \phi}{\partial \xi} - \phi &= 0, \\ \phi &= -\psi_I \quad \text{if } \xi = 0 \\ \lim_{\xi \rightarrow \infty} \phi &= 0, \end{aligned}$$

which can be deduced in a straightforward way from the detailed presentation of Munk's model in section 5.4 of Pedlosky [2]. Problem (8) has solutions of the kind

$$(9) \quad \phi = \phi(\xi, y, C(.)),$$

where $C(.)$ is a yet undefined function of y if $\delta_M > 0$, while no arbitrary function $C(.)$ comes into play if $\delta_M = 0$. From (9) we can evaluate the lowest-order meridional velocity within the western boundary layer

$$(10) \quad v^{(w)}(\xi, y; C(.)) = \frac{L}{\delta_F} \frac{\partial \phi}{\partial \xi},$$

and the integrated kinetic energy

$$(11) \quad K^{(w)}(C(.)) = \frac{1}{2} \int_0^1 dy \int_0^\infty d\xi v^{(w)}(\xi, y; C(.))^2.$$

In the next section we show that, for a suitable and unique function $C_0(.)$, the double implication

$$(12) \quad v^{(w)}(0, y; C_0(.)) = 0 \iff K^{(w)}(C_0(.)) = \min_{C(.)} K^{(w)}(C(.))$$

holds, while the existence of $C_0(\cdot)$ is granted by the linearity of (8). This means that choosing the no-slip condition (left side of (12)) is equivalent to minimizing the kinetic energy of the boundary layer (right side of (12)).

For comparison with the no-slip condition, we shall also consider the free-slip condition

$$(13) \quad \frac{\partial}{\partial \xi} v^{(w)}(\xi, y; C(\cdot)) = 0 \quad \text{at } \xi = 0 .$$

3. – Role of the relative boundary-layer width r

We preliminarily set, in short,

$$(14) \quad r = \frac{\delta_S}{\delta_M}$$

and consider separately the ranges

$$(15) \quad 0 \leq r \leq 1$$

and

$$(16) \quad 1 < r ,$$

which correspond to a large Munk layer and to a large Stommel layer, respectively.

3.1. Large Munk layer ($r \leq 1$)

3.1.1. Kinetic energy of the boundary layer. First, we assume (15). Because of (3) and (14), $\delta_F = \delta_M$ and hence problem (8) becomes

$$(17) \quad \begin{aligned} \frac{\partial^3 \phi}{\partial \xi^3} - r \frac{\partial \phi}{\partial \xi} - \phi &= 0 , \\ \phi &= -\psi_I \quad \text{if } \xi = 0 , \\ \lim_{\xi \rightarrow \infty} \phi &= 0 . \end{aligned}$$

For all r satisfying condition (15), the associated algebraic equation

$$(18) \quad \lambda^3 - r \lambda - 1 = 0$$

has one and only one real root, which is positive and hence does not yield a solution of (17). On the other hand, the two complex roots of this equation satisfy for all $r \in [0, 1]$ the condition $\text{Re } \lambda < 0$ demanded by the limit condition of (17). The leftmost part of fig. 1 shows Cartesian plots of all these roots as a function of r in the range (15). Introducing the magnitudes of the real and imaginary parts of λ through

$$(19) \quad p(r) = |\text{Re } \lambda(r)| \quad q(r) = |\text{Im } \lambda(r)|$$

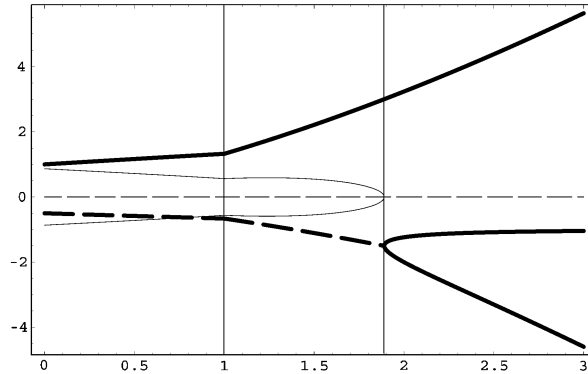


Fig. 1. – Cartesian plots of the roots of eqs. (18) and (36) as functions of relative boundary layer width r for $0 \leq r \leq 1$ and for $1 < r$, respectively. Thick continuous, thick dashed, and thin continuous curves represent real roots, real parts of complex roots, and imaginary parts of complex roots, respectively. The rightmost vertical line marks the critical value $r = (27/4)^{(1/3)} \simeq 1.9$. The thin dashed line represents the axis of abscissas.

the admissible solutions of (17) take the form

$$(20) \quad \phi = \exp[-p \xi][C(y) \sin(q \xi) - \psi_I(0, y) \cos(q \xi)] .$$

Here, evaluation of (10) with (20) yields the meridional velocity in the boundary layer

$$(21) \quad v^{(w)}(\xi, y; C(\cdot)) = \frac{L}{e^p \xi \delta_M} \{ [q C(y) + p \psi_I(0, y)] \cos(q \xi) - [p C(y) - q \psi_I(0, y)] \sin(q \xi) \}$$

and hence the meridional velocity along the western wall

$$(22) \quad v^{(w)}(0, y; C(\cdot)) = \frac{L}{\delta_M} [p \psi_I(0, y) + q C(y)] ,$$

while (11) evaluated with (20) gives the kinetic energy of the flow in the western boundary layer, *i.e.*

$$(23) \quad K^{(w)}(C(\cdot)) = \frac{L^2}{8 p \delta_M^2} \int_0^1 dy \left[(q C(y) + p \psi_I(0, y))^2 + (p^2 + q^2) \psi_I^2(0, y) \right] .$$

From (22) and (23) we see that the function

$$(24) \quad C_0(y) = -\frac{p}{q} \psi_I(0, y) \quad (\text{no-slip})$$

verifies (12) in the range (15) and that (24) is unique.

On the other hand, the free-slip condition (13) implies that $C(\cdot)$ be given by

$$(25) \quad C_{\text{free}}(y) = \frac{q^2 - p^2}{2 p q} \psi_I(0, y) \quad (\text{free-slip}) .$$

3.1.2. Example: sinusoidal variation of the forcing with latitude. Assuming sinusoidal variation of the wind stress with latitude in an idealized subtropical gyre, namely

$$(26) \quad \text{curl}_z \bar{\tau} = -\sin(\pi y) ,$$

we get from (5)

$$(27) \quad \psi_1(0, y) = \sin(\pi y) .$$

Therefore, from (24) and (25) we get

$$(28) \quad C_0(y) = -\frac{p}{q} \sin(\pi y) \quad (\text{no-slip})$$

and

$$(29) \quad C_{\text{free}}(y) = \frac{q^2 - p^2}{2pq} \sin(\pi y) \quad (\text{free-slip}) ,$$

respectively.

Moreover, the kinetic energy of the flow in the western boundary layer is readily computed; indeed, (27) and (28) imply

$$(30) \quad K^{(w)}(C_0(\cdot)) = \frac{L^2}{16 \delta_M^2} \frac{p^2 + q^2}{p} \quad (\text{no-slip}) ,$$

while (27) and (29) yield

$$(31) \quad K^{(w)}(C_{\text{free}}(\cdot)) = \frac{L^2}{64 \delta_M^2} \frac{(p^2 + q^2)(5p^2 + q^2)}{p^3} \quad (\text{free-slip}) .$$

To get further physical insight, we introduce the longitudinal distribution of the integrated kinetic energy (cf. (11))

$$(32) \quad K^{(w)}(\xi; C(\cdot)) = \frac{1}{2} \int_0^1 dy \int_0^\xi d\eta v^{(w)}(\eta, y; C(\cdot))^2$$

Figure 2 shows the integrated kinetic energy $K^{(w)}(\xi, C(\cdot))$ in the free-slip (thick curve) and in the no-slip (thin curve) case for $r = 0.2, 0.4, 0.6$ and 0.75 . Lower values of r correspond to higher values of $K^{(w)}$. The figure is in agreement with our previous analytical argument (see the end of the Introduction). Note also the different rate of energy increase in the proximity of the western wall.

The algebraic expressions that give p and q in terms of r are, in general, quite cumbersome. But, when $r = 3/4$ they result to be relatively simple:

$$(33) \quad p = \frac{1}{4} \left[\left(4 + \sqrt{15}\right)^{1/3} + \left(4 - \sqrt{15}\right)^{1/3} \right] \simeq 0.623 ,$$

$$(34) \quad q = \frac{\sqrt{3}}{4} \left[\left(4 + \sqrt{15}\right)^{1/3} - \left(4 - \sqrt{15}\right)^{1/3} \right] \simeq 0.644 .$$

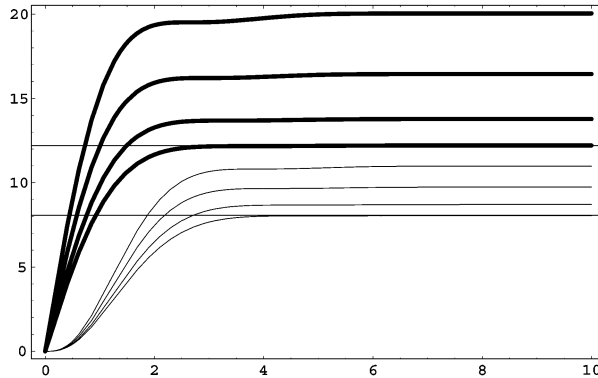


Fig. 2. – Cartesian plots of the integrated kinetic energy $K^{(w)}$ as a function of stretched coordinate ξ , when the relative boundary layer width takes the values $r = 0.2, 0.4, 0.6, 0.75$. No-slip (thin lines) and free-slip (thick lines) boundary conditions have been assumed. Lower values of r correspond to higher values of $K^{(w)}$. Equation (21) with $L/\delta_M = 10$ has been used for this graph. The horizontal lines correspond to $K^{(w)}(C_0(.)) = 8.05$ and $K^{(w)}(C_{\text{free}}) = 12.2$ (see text).

In this case, (30) and (31) yield, for $L/\delta_M = 10$, $K^{(w)}(C_0(.)) \simeq 8.05$ and $K^{(w)}(C_{\text{free}}(.)) \simeq 12.2$, respectively, in perfect agreement with the plots of $K^{(w)}(C(.))$ in fig. 2.

3'2. Large Stommel layer ($1 < r$). – Second, we assume (16), and problem (8) becomes

$$\begin{aligned}
 (35) \quad & \frac{1}{r^3} \frac{\partial^3 \phi}{\partial \xi^3} - \frac{\partial \phi}{\partial \xi} - \phi = 0, \\
 & \phi = -\psi_I \quad \text{if } \xi = 0, \\
 & \lim_{\xi \rightarrow \infty} \phi = 0.
 \end{aligned}$$

The roots of the algebraic equation

$$(36) \quad \frac{1}{r^3} \lambda^3 - \lambda - 1 = 0 \quad (1 < r)$$

associated to the vorticity equation (35)₁, are also depicted in fig. 1. Since Cardano formula for the previous equation involves $\sqrt{27/4 - r^3}$, it is useful to introduce the critical value $r_c = (27/4)^{1/3}$ and to take separately into account the following intervals:

$$(37) \quad 1 < r < r_c,$$

$$(38) \quad r = r_c,$$

$$(39) \quad r_c < r.$$

Finally, we shall pay special attention to the asymptotic limit $r \rightarrow \infty$, in which lateral diffusion of relative vorticity is vanishingly small with respect to bottom friction: it may be viewed as representative of a very thin sublayer ([2], section 5.5).

In the range (37), we ascertain two complex conjugate solutions with negative real part (see fig. 1), so the solution of (35) is still given by (20). Therefore (22) and (23) hold

good, but with δ_S in place of δ_M . The conclusion is exactly the same as that previously stated.

In case (38), the algebraic equation has one real negative root, namely $\lambda = -3/2$, with double multiplicity. This implies the following solution of (35):

$$(40) \quad \phi = \exp[-3\xi/2] [C(y)\xi - \psi_I(0, y)]$$

whence the velocity along the wall is

$$(41) \quad v^{(w)}(0, y, C(\cdot)) = \frac{L}{\delta_S} \left[C(y) + \frac{3}{2} \psi_I(0, y) \right]$$

and the kinetic energy is

$$(42) \quad K^{(w)}(C(\cdot)) = \frac{L^2}{12\delta_S^2} \int_0^1 dy \left[\left(C(y) + \frac{3}{2} \psi_I(0, y) \right)^2 + \frac{9}{4} \psi_I(0, y)^2 \right].$$

Equations (41) and (42) show that the function

$$(43) \quad C_0(y) = -\frac{3}{2} \psi_I(0, y)$$

verifies equivalence (12) and that (43) is unique.

In range (39), according to fig. 1, the algebraic equation has two real negative roots, namely $\lambda_1 = -a_1(r)$ and $\lambda_2 = -a_2(r)$. The solution of (35) is therefore

$$(44) \quad \phi = C(y) \exp[-a_1 \xi] - [C(y) + \psi_I(0, y)] \exp[-a_2 \xi].$$

Evaluation of (10) and (11) with (44) yields the velocity

$$(45) \quad v^{(w)}(0, y, C(\cdot)) = \frac{L}{\delta_S} [(a_2 - a_1) C(y) + a_2 \psi_I(0, y)]$$

and the kinetic energy

$$(46) \quad K^{(w)}(C(\cdot)) = \frac{L^2}{4(a_1 + a_2)\delta_S^2} \int_0^1 dy \left\{ [(a_2 - a_1) C(y) + a_2 \psi_I(0, y)]^2 + a_1 a_2 \psi_I(0, y)^2 \right\},$$

respectively. From (45) and (46) we see that the function

$$(47) \quad C_0(y) = \frac{a_2}{a_1 - a_2} \psi_I(0, y)$$

verifies equivalence (12) in the range $r_c < r$, and that (47) is unique.

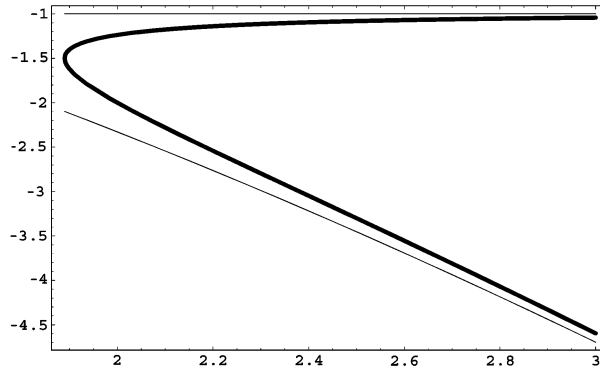


Fig. 3. – Asymptotic behavior of the negative roots of eq. (36) as functions of relative boundary layer width r . Thick and thin curves represent exact roots and their asymptotic approximations, respectively.

In the limit case $r \rightarrow \infty$ we may state, roughly speaking, that *the limit of the solution is the solution of the limit equation*, if the no-slip condition has been chosen. More precisely, for $r \rightarrow \infty$, eq. (35)₁ becomes

$$(48) \quad \frac{\partial \phi}{\partial \xi} + \phi = 0$$

and its solution with boundary conditions (35)_{2,3} is uniquely given by

$$(49) \quad \phi = -\psi_1(0, y) \exp[-\xi] .$$

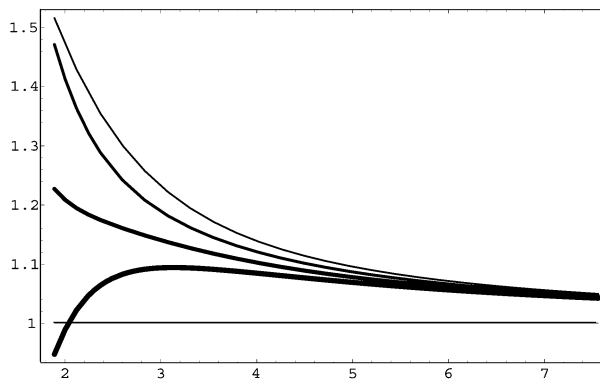


Fig. 4. – Cartesian plot of the ratio between solution (44) and trivial solution (49) vs. relative boundary layer width r . Each curve is related to a different value of the stretched coordinate $\xi = 1, 2, 3, 4$. Thicker lines correspond to higher values of ξ .

On the other hand, we may assume $a_1 < a_2$ and rearrange solution (44) as

$$(50) \quad \phi = C(y) \exp[-a_1 \xi] \left\{ 1 - \left[1 + \frac{\psi_I(0, y)}{C(y)} \right] \exp[-(a_2 - a_1) \xi] \right\},$$

which approaches (49) for $r \rightarrow \infty$, if $C = C_0$ given by (47), since (see fig. 3)

$$(51) \quad a_1(r) = 1 + O(r^{-3/2}),$$

$$(52) \quad a_2(r) = r^{3/2} - 1 + O(r^{-3/2})$$

and hence

$$(53) \quad \lim_{r \rightarrow 0} C_0(y) = -\psi_I(0, y).$$

This phenomenon is illustrated in fig. 4.

3.3. Kinetic energy in the presence of no-slip condition. – In all the considered cases of no-slip conditions, a relationship of the kind

$$(54) \quad K^{(w)}(C_0(\cdot)) = \alpha \int_0^1 dy \psi_I(0, y)^2$$

holds, where the form of α results from the following table:

α	Equation	Condition
$L^2 (p^2 + q^2)/(8 \delta_M^2 p)$	(23)	$r \leq 1$
$L^2 (p^2 + q^2)/(8 \delta_S^2 p)$	—	$1 < r < r_c$
$3 L^2 / (16 \delta_S^2)$	(42)	$r = r_c$
$L^2 a_1 a_2 / [4 (a_1 + a_2) \delta_S^2]$	(46)	$r_c < r$

Then, substitution of (5) into (54) gives

$$(55) \quad K^{(w)}(C_0(\cdot)) = \alpha \int_0^1 dy \left[\int_0^1 dx \operatorname{curl}_z \bar{\tau}(x, y) \right]^2.$$

The integral on the r.h.s. of (55) is independent of any boundary condition and it gives the minimum energy of the flow in the western boundary layer in terms of the forcing field. In particular, (55) shows that the kinetic energy of the western boundary layer is zero only if

$$(56) \quad \int_0^1 dx \operatorname{curl}_z \bar{\tau}(x, y) = 0$$

as Rhines and Young [8] assumed in an artificial, but elucidating, example. This happens simply because, in case (56), the wind-stress curl forces the flow in the whole basin partly southward and partly northward, without need of any boundary layer to close the circulation patterns.

4. – Concluding remarks

The main result of the present investigation is the double implication (12), which holds for any value of the relative boundary layer width r defined by (14). It may be phrased in plain words by saying that choosing the no-slip condition is equivalent to minimizing the kinetic energy of the boundary layer.

From the perspective of the boundary layer theory, we have seen how every dynamic boundary condition determines a definite amount of kinetic energy in the western boundary layer. But, we may safely assume that no boundary condition produces, because of its own nature, a physical source of energy. Then any fictitious surplus of energy, besides the “fundamental” quantity reported in (55), can be eliminated by imposing the no-slip boundary condition along the western wall of the basin. However, these conclusions suffer from some limitations, which we put forward in what follows.

- Linearity is an essential hypothesis, since boundary layer solutions are not necessarily found in the presence of nonlinearity, as Ierley and Ruehr [9] have shown.
- If superslip or hyperslip conditions are applied to the flow, no boundary layer solution is possible and the circulation problem must be solved as a whole. Details can be found, for instance, in Carnevale *et al.* [10] in the case of the superslip condition at the western wall and free-slip elsewhere.
- Marshall [11] has obtained quite different and very interesting results from unsteady double-gyre quasi-geostrophic eddy resolving simulations, in which counter rotating gyres can laterally exchange properties. In fact, a double-gyre calculation demonstrates that a vorticity equilibrium with extensive Sverdrup interiors is possible without recourse to frictional boundary layers. The unstable internal eastward jet at the border of the counter rotating gyres exchanges all the required vorticity to attain equilibrium. It is therefore evident that conclusions highly depend on the considered model.

* * *

FC is very grateful to Prof. J. PEDLOSKY for an interesting discussion on the sublayer dynamics and to Dr. G. BADIN for providing him with the paper of J. C. MARSHALL.

REFERENCES

- [1] BATCHELOR G. K., *An Introduction to Fluid Dynamics* (Cambridge University Press) 1967.
- [2] PEDLOSKY J., *Geophysical Fluid Dynamics* (Springer-Verlag) 1987.
- [3] KAMENKOVICH, V. M., KOSHLYAKOV M. N. and MONIN A. S., *Synoptic Eddies in the Ocean* (D. Reidel Publishing Company) 1986.
- [4] MC WILLIAMS J. C., *Ocean modelling and parameterization* edited by P. ERIC CHASSIGNET and J. VERRON, *NATO Science Series, Series C*, Vol. **516** (1998).
- [5] PEDLOSKY J., *Ocean Circulation Theory* (Springer-Verlag) 1996.
- [6] CASTELLANA L., CRISCIANI F. and PURINI R., *Nuovo Cimento C*, **24** (2001) 377.
- [7] CRISCIANI F., *Eur. Phys. J. B*, **31** (2003) 571.
- [8] RHINES P. B. and YOUNG W. R., *J. Mar. Res.*, **40** (Supplement) (1982) 559.
- [9] IERLEY G. R. and RUEHR O. G., *Studies in Appl. Math.*, **75** (1986) 1.
- [10] CARNEVALE G. F., CAVALLINI F. and CRISCIANI F., *J. Phys. Oceanogr.*, **31** (2001) 2489.
- [11] MARSHALL J. C., *On the treatment of the lateral boundary in large-scale ocean models* 1983 (unpublished paper).